PROCEEDINGS OF SCIENCE

# Medium Modification of Meson Masses

**Jochen Wambach***
*Institut für Kernpysik, Technical University Darmstadt, D-64289 Darmstadt, Germany*
*and*
*Gesellschaft für Schwerionenforschung, D-64291 Darmstadt, Germany*
*E-mail:* j.wambach@gsi.de

I review pertinent aspects of the phase structure of strongly interacting matter and their relation to the medium modifications of mesons. Special attention is paid to the critical endpoint in the phase diagram and the electromagnetic response in its vicinity.

*Critical Point and Onset of Deconfinement 4th International Workshop*
*July 9-13 2007*
*GSI Darmstadt,Germany*

*Speaker.





PoS(CPOD07)039

## 1. Introduction

The prime objective of ultra-relativistic heavy-ion collisions is to create equilibrated strongly-interacting matter under extreme conditions in temperature and density. Fig. 1 shows a schematic view of our present understanding of the phase diagram, which is based on QCD-inspired models and ab-initio predictions from lattice simulations of the QCD partition function. The rich struc-

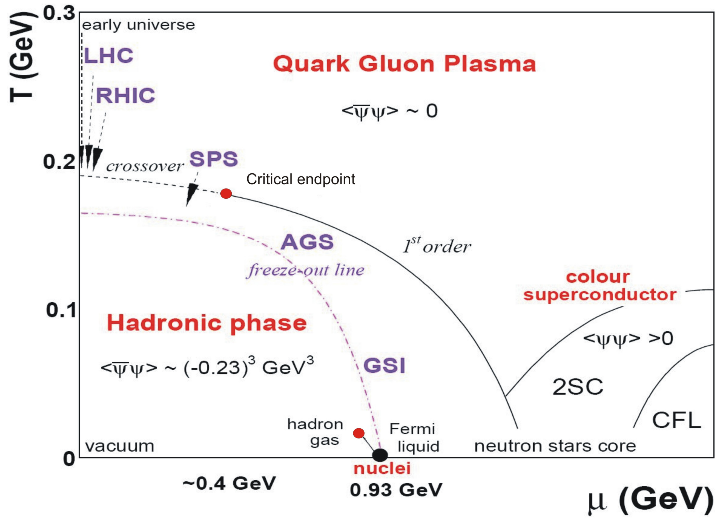


**Figure 1:** A schematic view of the QCD phase diagram as it is perceived today

ture is in part due to the fact that besides confinement, QCD exhibits (an almost exact) chiral $SU(2)_L \times SU(2)_R$ symmetry in the sector of $u$ and $d$ quarks. In the confined hadronic phase this symmetry is spontaneously broken to the vectorial subgroup $SU(2)_V$ leading to a non-vanishing chiral condensate of quark-antiquark pairs, $\langle \bar{q}q \rangle$, the mass generation for (constituent) quarks with $M_q \sim 300\,\text{MeV} \sim \Lambda_{QCD}$, bound color-neutral quark-antiquark pairs in the form of mesons as well as baryons consisting of 3 valence constituent quarks. At the same time also the gluons condense with a finite vacuum expectation value for the squared gluon field-strength tensor, $\langle (gG^a_{\mu\nu})^2 \rangle \equiv \langle G^2 \rangle$.

The particular interest of this workshop is the possible existence of a critical endpoint (CEP) as predicted on the basis of model calculations [1] as well as lattice QCD simulations [2, 3, 4]. Similar to water, this is the endpoint of a first-order (chiral) transition line in the $(T, \mu_q)$-plane and is a genuine singularity of the QCD free energy. At the CEP the phase transition is of second order, belonging to the universality class of the three-dimensional Ising model. Both the chiral susceptibility $\chi_m = \partial^2 p/\partial m_q^2$ and the quark-number susceptibility $\chi_q = \partial^2 p/\partial \mu_q^2$ diverge at the CEP. It might be accessible with current and future experimental facilities such as the "Compressed Baryon Matter" (CBM) experiment at FAIR and its observable implications in relativistic heavy-ion experiments, such as event-by-event fluctuations of suitable observables or possible signals in dilepton pair production, are intensively discussed [5]. The precise location of the CEP, which is highly sensitive to the value of the strange-quark mass, is not known at present. Lattice calculations with finite $\mu_q$ are difficult due to the Fermion sign problem. From direct numerical evaluation of the partition function and its quantum-statistical analysis [2, 3] or from a Taylor expansion of the pressure around $\mu_q = 0$ [4] it has been attempted to pin down the location of the CEP but the results remain highly uncertain.

## 2. The electromagnetic response of hot and dense matter

As the phase boundary is approached from the confined phase, strong medium modifications of hadrons are expected. More than 90 % of the constituent mass, $M_q$, of light up and down quarks is generated by spontaneous chiral symmetry breaking in the vacuum ($M_q \propto m_q + \langle \bar{q}q \rangle$). As the chiral condensate diminishes with temperature and density (Fig. 2), $M_q$ decreases approaching the bare quark mass, $m_q$, as the symmetry gets restored.

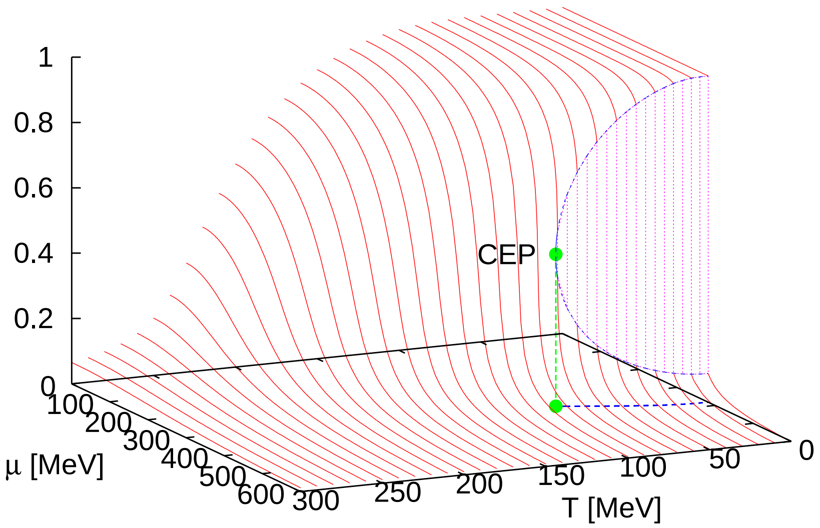


**Figure 2:** Evolution of the chiral condensate with $T$ and $\mu_q$ in the Nambu Jona-Lasinio (NJL) model. First-order transitions at small temperatures and large chemical potentials are clearly visible, finally ending in the CEP.

Since hadrons consist of constituent quarks, their masses should also change (most naively their mass evolution should follow that of $M_q$ which is usually called the 'dropping mass scenario' [6]). The situation is however more complicated, since there are residual correlations between the constituent quarks. This can be seen explicitly in the NJL model and has been known for a long time[7]. Therefore, more generally, one is interested in the changes of the spectral properties (shifts in the pole mass and modifications of the decay width through new decay channels).

An ideal tool for diagnosing changes in the spectral properties is the measurement of real or virtual photons in heavy-ion collisions. Photons have a mean-free path of $10^2 - 10^4$ fm, which is large compared to the size of the fireball. Thus they illuminate all stages of the collision, from initial hard radiation to the final hadronic decays after thermal freeze out. Assuming (local) thermal equilibrium, the principal quantity probed is the (retarded) electromagnetic correlator of the medium

$$D^{\mu\nu}_{elm}(\omega,\vec{q}) = -i\int d^4x\,\Theta(t)e^{i(\omega t-\vec{q}\cdot x)}\langle\langle j^{\mu}_{elm}(x)j^{\nu}_{elm}(0)\rangle\rangle \ . \tag{2.1}$$

Here

$$j^{\mu}_{elm}(x) = \sum_i e_i\bar{q}_i(x)\gamma^{\mu}q_i(x) \tag{2.2}$$

denotes the elm current in terms of quark fields and the average is taken in the grand-canonical ensemble. In the medium, Lorentz invariance is broken. This has two consequences: 1. $\omega$ and $\vec{q}$ become independent variables where $M^2 = \omega^2 - \vec{q}^2$ is the invariant mass$^2$, 2. the correlator has both longitudinal and transverse components

$$D^{\mu\nu}_{elm} = D_L P^{\mu\nu}_L + D_T P^{\mu\nu}_T \tag{2.3}$$

where $P^{\mu\nu}_{L/T}$ are kinematic projectors. The scalar functions $D_{L/T}$ have a spectral representation,

$$D_{L/T}(\omega,\vec{q}) = \int_0^{\infty} d\omega'^2 \frac{\rho_{L/T}(\omega',\vec{q})}{\omega'^2-\omega^2+i\varepsilon} \tag{2.4}$$

and the physical information about the system is contained in these spectral functions $\rho_{L/T}(\omega,\vec{q})$. The local rates for real photons or dileptons in given space-time volume are obtained by contracting the elm tensor (2.1) with the leptonic tensor and one obtains

$$\begin{aligned}\omega\frac{dN_\gamma}{d^3q} &= \frac{\alpha}{\pi}\frac{1}{e^{\omega/T}-1}\rho^L_{\rm elm}(\omega=|\vec{q}|)\\ \frac{dN_{l^+l^-}}{d^4q} &= \frac{\alpha^2}{\pi^2M^2}\frac{1}{e^{\omega/T}-1}\left(\frac{1}{3}\rho^L_{\rm elm}(\omega,\vec{q})+\frac{2}{3}\rho^T_{\rm elm}(\omega,\vec{q})\right)\end{aligned} \tag{2.5}$$

Finally the total rate is obtained by integrating the local rate over the space-time evolution of the collision.

From $e^+e^- \to$ hadrons data it is well known that, in the vacuum, the low invariant mass ($M \lesssim$ 1 GeV) elm spectral function is dominated by light vector mesons with the $\rho$ meson being the most important contribution due to its quark-charge composition. (Fig. 3)

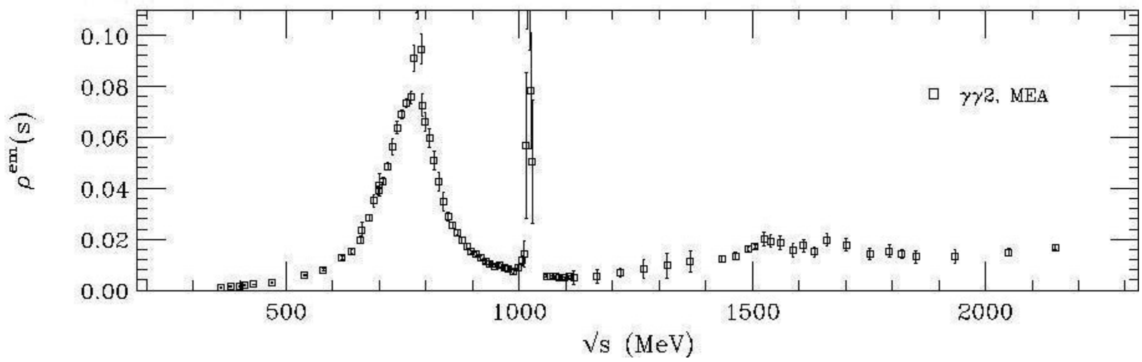


**Figure 3:** Electromagnetic spectral function of the vacuum as measured in $e^+e^-$ annihilation. The ratio $R^h(s) = \frac{\sigma(e^+e^-\to\text{hadrons})}{\sigma(e^+e^-\to e^+e^-)}$ is plotted as a function of the cms energy

A useful theoretical approach is therefore vector-meson dominance (VMD) [8] in which the elm current is expressed by the current-field identity

$$j^{\mu}_{elm} = -\frac{e}{g_\rho} m^2_\rho \rho^\mu - \frac{e}{g_\omega} m^2_\omega \omega^\mu - \frac{e}{g_\phi} m^2_\phi \phi^\mu \; . \tag{2.6}$$

Considering the $\rho$ meson we then have

$$D^{\mu\nu}_{elm} \propto \langle\langle \rho^\mu \rho^\nu \rangle\rangle \to \mathrm{Im} D^{\mu\nu}_\rho \; . \tag{2.7}$$

The effective Lagrangian includes the coupling to pions and is given by

$$\begin{aligned} \mathscr{L}_{VDM} &= \frac{1}{2}(D_\mu \vec{\pi})^2 - \frac{1}{2} m^2_\pi \vec{\pi}^2 - \frac{1}{4}\rho_{\mu\nu}\rho^{\mu\nu} + \frac{1}{2} m^2_\rho \rho_\mu \rho^\mu \\ \rho_{\mu\nu} &= \partial_\mu \rho_\nu - \partial_\nu \rho_\mu ; \qquad D_\mu \vec{\pi} = (\partial_\mu - i g \rho_\mu \tau_3)\vec{\pi} \; . \end{aligned} \tag{2.8}$$

By adjusting the coupling constant $g$, excellent agreement with data, such as the time-like elm formfactor of the pion and the $p$-wave $\pi\pi$-scattering phase shifts, are obtained at the one-loop level.

In the hadronic medium the $\rho$-meson propagator is expressed in terms of longitudinal and transverse self energies

$$D^{\mu\nu}_\rho = -\frac{P^{\mu\nu}_L}{q^2 - m^2_\rho - \Sigma_L} - \frac{P^{\mu\nu}_T}{q^2 - m^2_\rho - \Sigma_T} - \frac{q^\mu q^\nu}{m^2_\rho q^2} \tag{2.9}$$

which encode the medium effects. In hadronic many-body theory [9] (HMT) these are calculated from effective interactions integrated over the momentum distributions of mesons ($\pi, K, \rho..$) and baryons ($N, \Delta, N*, ..$) in the heat bath. The interaction vertices are compatible with gauge and chiral invariance and are constrained by resonance decay widths and scattering data in the vacuum. In the low-density limit, the photoabsorption cross section for the nucleon is well reproduced [9] (left panel of Fig. 4). Typical results for the in-medium $\rho$-meson spectral function are shown in the

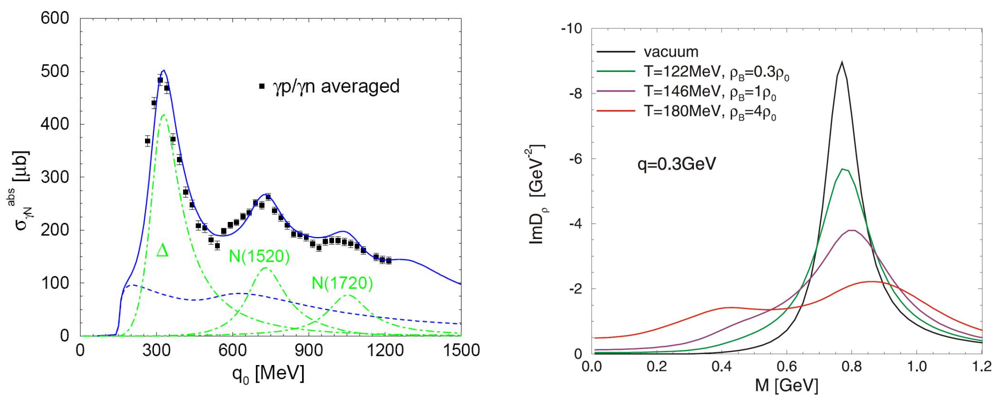


**Figure 4:** Left panel: total photoabsorption cross section on the nucleon as the low-density limit of the HMT [9]. Right panel: $\rho$-meson spectral function in hot hadronic matter at fixed $\mu_B = 3\mu_q = 330$ MeV (corresponding to CERN-SPS conditions).

right panel of Fig. 4. Prominent features are a strong broadening with little mass shift, mostly resulting from baryonic effects. When approaching the phase boundary, the $\rho$-meson spectral function 'melts' and resembles in form and magnitude that of the perturbative $\bar{q}q$ elm correlator. The measured dilepton yield of the NA60 collaboration [10] (left panel of Fig. 5) and the CERES

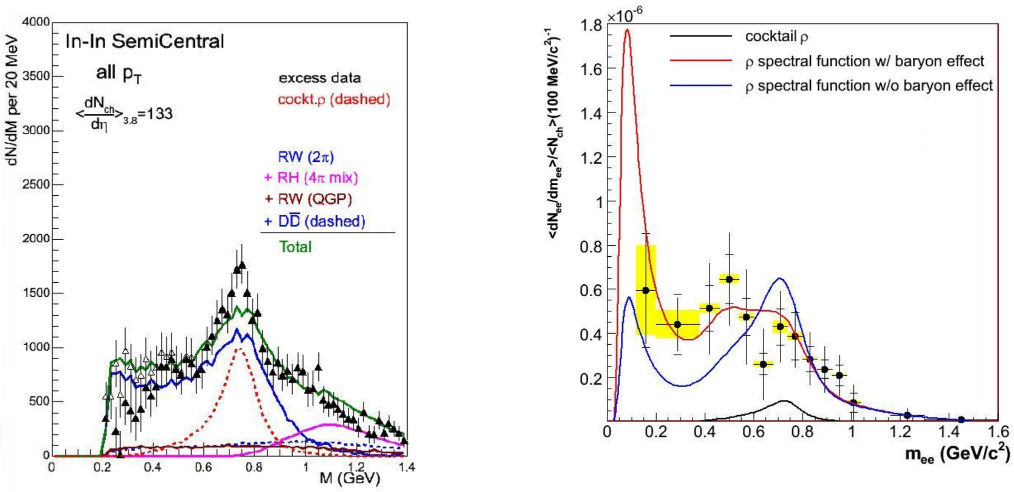


**Figure 5:** Dilepton yield after subtraction of the 'cocktail' contributions from $e^+e^-$ decays after thermal freeze out as measured by the NA60 collaboration [10] (left) and the CERES collaboration [11] (right).

collaboration [11] (right panel of Fig. 5) after subtraction of the hadronic 'cocktail' contributions are well reproduced by the HMT, but only if baryonic effects are included. This is illustrated in the right panel of Fig. 5, which compares the calculation with and without baryonic effects. The latter case is clearly ruled out by the data. Also the 'dropping mass' scenario, in which the $\rho$-meson pole mass drops with density and temperature is not supported.

## 3. Electromagnetic signals near the CEP

In the $\rho$(isovector)-channel the restoration of chiral symmetry seems manifest itself in a strong broadening of the response, going over smoothly into the perturbative quark limit. Let us consider the isoscalar quark current

$$j^{\mu}_{I=0} = \bar{q}(x)\gamma^{\mu}q(x) \tag{3.1}$$

instead. It has the same quantum numbers as the $\omega$ meson (vector-isoscalar). The $0^{th}$ component of $j^{\mu}_{I=0}$ is the quark number density, $n_q(x) = q(x)^{\dagger}q(x)$. Another quantity of interest is the scalar density $n_m(x) = \bar{q}(x)q(x)$, which is a scalar isoscalar ($\sigma$ meson). Both densites are order parameters for the quark-hadron transition near the CEP, i.e. in the Landau Ginzburg sense the thermodynamic potential, $\Omega$, can be expressed in terms of both quantities. At finite $\mu_q$ and $T$ the scalar ($\sigma$) and density ($\omega$) mode mix and at the CEP $\Omega$ becomes flat in the $\sigma$ as well as in the $\omega$ direction (Fig. 6). As a consequence the chiral susceptibility, $\chi_m$ and the quark-number susceptibility $\chi_q$ diverge:

$$\chi_m = -\frac{\partial^2\Omega}{\partial m_q^2}, \quad \chi_q = -\frac{\partial^2\Omega}{\partial \mu_q^2} \quad \to \infty\ . \tag{3.2}$$

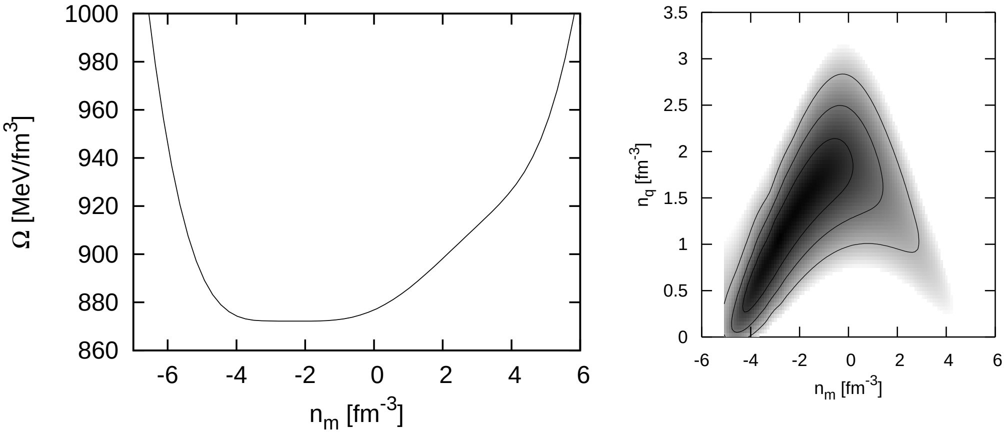


**Figure 6:** Left panel: The thermodynamic potential at the CEP in the $\sigma$ dircation Right panel: contours of $\Omega$ in the $n_q$ and $n_m$ directions.

This behavior is encoded in the spectral properties of the density correlation function (longitudinal part of the $\omega$-meson spectral function)

$$D_{n_q}(\omega,\vec{q}) = -i\int d^4x\,\Theta(t)e^{i(\omega t-\vec{q}\cdot x)}\langle\langle n_q(x)n_q(0)\rangle\rangle \propto D^L_\omega(\omega,\vec{q}) \tag{3.3}$$

as well as the scalar correlation function ($\sigma$ spectral function)

$$D_{n_m}(\omega,\vec{q}) = -i\int d^4x\,\Theta(t)e^{i(\omega t-\vec{q}\cdot x)}\langle\langle n_q(x)n_q(0)\rangle\rangle \propto D_\sigma(\omega,\vec{q}) \tag{3.4}$$

Since

$$\chi_i = \lim_{\vec{q}\to 0} D_i(0,\vec{q}) = \lim_{\vec{q}\to 0}\int_0^\infty d\omega'^2\,\frac{\rho_i(\omega',\vec{q})}{\omega'^2+i\varepsilon} \tag{3.5}$$

this implies that both the $\sigma$ and the longitudinal $\omega$ spectral functions soften in the vicinity of the CEP for space-like four momenta and the strength is concentrated at $\omega = 0$ right at second-order phase transition. This is illustrated in Fig. 7, which shows the spectral functions in the scalar and density channel, calculated in the NJL model [12]. An interesting question is whether the space-like mode softening can also be observed in the time-like region, as probed by dilepton production in heavy-ion collisions. Since the $\sigma$ mode softens [13] one might observe a strong downward shift of the $\omega$-part of dilepton rate. In the NJL calculation shown in Fig. 7 there seems to be little indication. This may, however, be artifact of the mean-field approximation and the lack of explicit inclusion of vector degrees of freedom. This is currently under investigation [14].

## 4. Summary and Conclusions

Of particular interest is the possible occurrence of a critical endpoint at finite $T$ and $\mu_q$, at which a line of first-order chiral transitions ends in a second-order transition. The determination of the precise location of this point in the $(T,\mu_q)$ plane and the size of the critical region [15] are

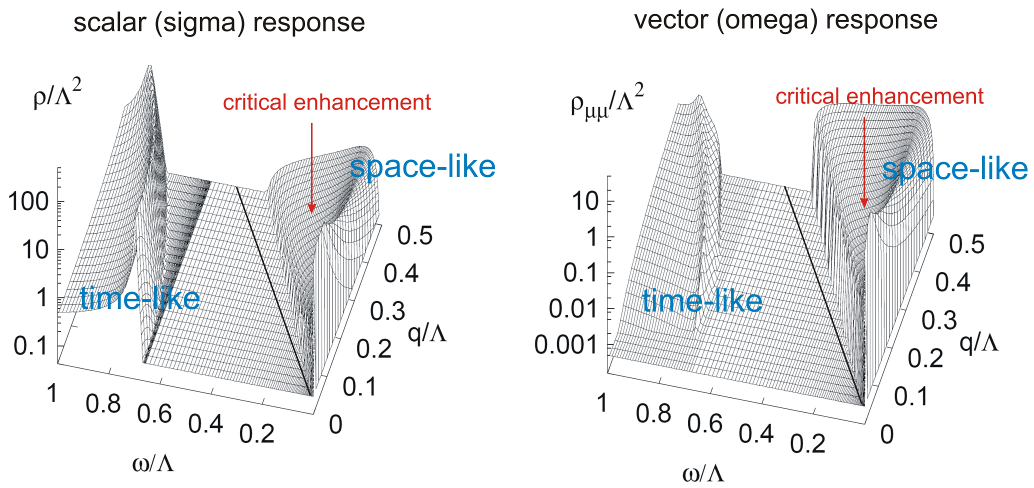


**Figure 7:** Left panel: scalar ($\sigma$) spectral function in the NJL model [12] near the CEP. Right panel: density (longitudinal $\omega$) spectral function.

of great importance for heavy-ion experiments since the critical behavior may be measurable, e.g. in event-by-event fluctuations or dilepton production. I have discussed the in-medium properties of the $\rho$ meson which is a prominent part of the (low-mass )dilepton yield in heavy-ion collisions. The modified spectral function calculated in hadronic many-body theory, which predicts significant broadening, accounts quantitatively for the data and a dropping mass scenario [6] is ruled out. While presumably the isovector elm response ($\rho$) shows no sign of criticality in the vicinity of the CEP, this may be different in the isoscalar channel ($\omega$). From universality arguments and explicit model calculations it is known, that the space-like part of the longitudinal $\omega$ spectral function is strongly modified, showing critical enhancement of the low-frequency response. Whether such criticality is also observable in the time-like region remains to be seen.

## Acknowledgements

This work was supported in part by the grant from the BMBF under 06DA116..

## References


[1] A. Barducci et al., Phys. Rev. D **41** (1990), 1640.

[2] Z. Fodor and S. D. Katz, Phys. Lett. B **534** (2002), 87.

[3] P. de Frocrand and O. Phillipsen, Nucl. Phys. B **642** (2002), 290.

[4] C. R. Allton et al., Phys. Rev. D **68** (2003), 014507.

[5] M. A. Stephanov, Prog. Theor. Phys. Suppl **153** (2004), 139.

[6] G.E. Brown and M. Rho, Phys. Rev. Lett. **75** (1991), 2720; Phys. Rep. **269** (1996), 333.

[7] T. Hatsuda and T. Kunihiro, Phys. Rev. Lett. **55** (1985), 158; Phys. Rep. **247** (1994), 221.

[8] J.J. Sakurai, Ann. Phys. **11** (1960), 1.

[9] R. Rapp and J. Wambach, Adv. Nucl. Phys. **25** (2000), 1.

[10] NA60 Collaboration [R. Arnaldi et al.] Phys. Rev. Lett. **96** (2006), 162302.

[11] CERES Collaboration [D. Adamova et al.] arXiv:nucl-ex/0611022.

[12] H. Fujii and M. Ohtani, Phys. Rev. **D70** (2004) 014016.

[13] Z. Aouissat et al., Nucl. Phys. **A581** (1995) 471.

[14] D. Müller, M. Buballa and J. Wambach, work in progress.

[15] B.-J. Schaefer and J. Wambach, arXiv:hep-ph/0603256, Phys. Rev. D, in print.